# Effect of Adsorption on the Optimal Displacement of Acidic Crude Oil by Alkali

Recovery of acidic crude oil from porous media can be enhanced by injection of alkaline agents. For this process we have analyzed the detrimental effect of alkali adsorption on the mineral surface. The model, which is an extension of our earlier inert solid model, was formulated by conserving three independent species. The previous solution procedure is shown to fail and a new analysis of composition paths is necessary. By introducing the notion of critical point, a short-cut procedure is developed.

The predicted profiles and effluent histories are discussed. A new result is that adsorption on the solid surface could change the *ultimate* recovery even for an infinite slug of alkali due to the reduced influence of the optimal region in displacing oil. Further, the influence of a favorable viscosity ratio in displacing oil is also shown to be reduced by adsorption.

**T. S. Ramakrishnan**
**D. T. Wasan**
Department of Chemical Engineering
Illinois Institute of Technology
Chicago, IL 60616

## Introduction

The injection of alkaline agents into permeable media to enhance recovery of *acidic* crude oil is termed as the high-pH injection/flooding process. Surfactants generated *in situ* due to the neutralization of the acid by the alkali is largely responsible for the enhanced recovery. To describe this method of stimulated waterflooding, a fractional flow model was developed by Ramakrishnan and Wasan (1989). Although their model accounted for alkali/acid interactions along with relative permeability variations due to capillary number changes, the solid surface was considered to be chemically inert. Thus, chemical reactions of the pore fluids with the reservoir rock was unaccounted for. The solution to the simplified model indicated that for favorable viscosity ratios the low interfacial tension region at intermediate sodium concentrations (optimal region) ensures a substantial recovery of oil, despite a comparatively high interfacial tension value between a solution of *injection composition* and the crude oil.

The purpose of the present study is to consider mineral/alkali interactions and identify whether they affect the influence of the optimal region in recovering oil. It is shown that a straightforward extension of the inert solid model analysis is not possible due to changes in the mathematical nature of the solution. An alternative procedure that permits the construction of mathematically and physically admissible solution is therefore employed.

Despite the fact that the study of rock/alkali interactions is important for a successful design of high-pH flooding, this aspect of the process remains inadequately quantified. A major reason is that the mineralogy and the lithology of naturally occurring porous media are complex.

The number of possible mineral/alkali reactions is considerable. It is possible, however, to broadly classify them according to both the *reversibility* and the *rapidity* of the reactions. The *major* reversible reaction is the sodium/hydrogen ion exchange (Bunge, 1982). This reaction is rapid (Lieu *et al.*, 1982) and contributes to a chromatographic type of lag in the alkaline front (Bunge, 1982). In addition, a reversible Ca-Na ion exchange is possible. This releases $Ca^{2+}$ and can cause precipitation of $Ca(OH)_2$; these reactions have also been assumed to be rapid (Bunge and Radke, 1982). In contrast, slow reaction rate processes also occur, as the experimental studies by many other investigators have shown (Bunge and Radke, 1982; Sydansk, 1982; Dehghani and Handy, 1984; Mohnot *et al.*, 1985; Lieu *et al.*, 1985). These studies suggest that reservoir silicate materials can undergo slow dissolution that can become important over typical reservoir time scales. Although dissolved silica can act as a buffer, thus contributing to alkalinity in spite of caustic

T. S. Ramakrishnan is currently with Schlumberger-Doll Research, Ridgefield, CT 06877. Correspondence concerning this paper should be addressed to D. T. Wasan.

consumption (Mohnot *et al.*, 1985) when Al-containing minerals are present, aluminosilicates may precipitate. This precipitation, it appears, leads to irreversible hydroxide consumption (Mohnot *et al.*, 1985). Simultaneously, slow mineral dissolution reactions leading to the presence of $Ca^{2+}$, $Mg^{2+}$, $SO_4^{2-}$, and $CO_3^{2-}$ can also occur (Lieu *et al.*, 1985). Subsequently, they can cause $Ca(OH)_2$, calcium, and magnesium silicates to precipitate.

The vast array of reversible and irreversible, slow and fast reactions suggest that extensive studies are required to arrive at a reasonable quantification of mineral/alkali interactions. Needless to say, the crude oil/alkali reactions also lead to products that can react with many of the components due to mineral dissolution. In view of a great amount of uncertainty involved and to keep mathematics within the scope of analysis, we consider the major mineral/alkali interaction for which quantitative relationships are available. This is the sodium/hydrogen weak ion exchange. As observed by deZabala *et al.* (1982), despite the reversibility of this reaction, its rapidity causes a chromatographic delay that retards the onset of oil production and increases water to oil ratio in the produced fluid. The purpose of this paper is not to reemphasize their earlier conclusions, but mainly to find whether the conclusion of Ramakrishnan and Wasan (1989) regarding the role of low interfacial tension at intermediate sodium concentrations is altered in any way. Any alteration will have serious implications in the design of the injection process.

Complementing the practical importance in including mineral/alkali reversible interaction is the mathematical solution of the process. Our analysis shows that naive graphical constructions based on the Buckley-Leverett ideas are inadequate. Therefore, explicit discontinuity curve constructions are necessary to obtain the necessary profiles and history. It is found that the equations for the discontinuity curves introduce the notion of critical point which can be exploited in developing simple numerical procedures. In fact, the critical point is crucial to obtaining the composition route. In addition, the physical conclusion of the model relies on the existence of the critical point, since adsorption reduces not only the rate of oil production but also the ultimate amount of oil recovered, in spite of injecting an infinite slug of alkali.

## Alkali/Acid Interaction Equilibria

Interactions among the acids in the crude oil and the NaOH in the flood water have to be known before we write the conservation equations for the different components present in the system. The alkali/acid reaction equilibria have been discussed in detail by Ramakrishnan and Wasan (1983, 1989) and are described here for the purpose of completeness.

The acids in the crude oil are represented by a single-component HA whose distribution between the oleic and aqueous phases is represented by

$$K_D = \frac{C_{HA_o}}{C_{HA_w}}. \tag{1}$$

where $o$ and $w$ denote oil and water; $C_i$, the concentration $i$; $K_D$, the distribution ratio, which has typically a value of $10^4$. The dissociation of acid in the aqueous phase is given by $HA_w + H_2O \rightleftarrows H_3O^+ + A^-$, the corresponding dissociation constant being

$$K_A = \frac{(C_{H_3O^+})(C_{A^-})}{C_{HA_w}}. \tag{2}$$

Addition of alkali in the aqueous phase leads to a reduction in $H_3O^+$ governed by

$$K_w = (C_{H_3O^+})(C_{OH^-}), \tag{3}$$

where $K_w$ is the dissociation constant for water. The repartitioning of the species A to the oil phase is described by $Na^+ + A^- \rightleftarrows NaA_w$, and $NaA_w \rightleftarrows NaA_o$, where the equilibrium constants satisfy

$$K_{s1} = \frac{(C_{Na^+})(C_{A^-})}{C_{NaA_w}} \gg 1, \tag{4}$$

$$K_{s2} = \frac{(C_{NaA_w})}{(C_{NaA_o})} \ll 1, \tag{5}$$

and

$$K_s = K_{s1}K_{s2} = \frac{(C_{Na^+})(C_{A^-})}{C_{NaA_o}}. \tag{6}$$

The redissolution of species $A$ causes the interfacial tension to rise above a certain concentration of NaOH in batch systems. This intermediate concentration may therefore be termed "optimum" for high pH flooding.

## Mineral/Alkali Adsorption Isotherm

With the mineral site labeled $\overline{M}$, the reversible exchange can be modeled as (Bunge and Radke, 1982)

$$\overline{M} - H + Na^+ + H_2O \rightleftarrows \overline{M} - Na + H_3O^+.$$

Bunge (1982) measured hydroxyl ion consumption through this reversible reaction for Wilmington field sand and found that the adsorption isotherm representing *hydroxide consumption* was Langmuirian at a *given* NaCl concentration. The isotherm she obtained may be written as

$$\frac{\overline{n}_{Na}}{\overline{n}_\infty(C_2, T)} = \frac{K_r(C_2, T)(C_{Na^+} - C_2)}{1 + K_r(C_2, T)(C_{Na^+} - C_2)}, \tag{7}$$

where $\overline{n}_{Na}$ is the adsorbed Na in moles per unit volume of solid that leads to hydroxide consumption (Na adsorbed in excess of that due to NaCl), and $\overline{n}_\infty$ is the saturation adsorption. Here both $\overline{n}_\infty$ and the exchange equilibrium constant $K_r$ are assumed to be functions of $C_{Cl^-}$ and $T$, temperature. By keeping the initial concentration of NaCl the same as the injection concentration, we are justified in using $C_{Cl^-}$ as *parameter* $= C_2$. The adsorption isotherm given by Eq. 7 expresses $\overline{n}_{Na}$ in terms of $C_{Na^+} - C_2$ rather than $C_{OH^-} - C_{H_3O^+}$ as proposed by Bunge (1982) and Bunge and Radke (1982) only to reflect the nature of the adsorption ion exchange. From a charge balance, it is seen that

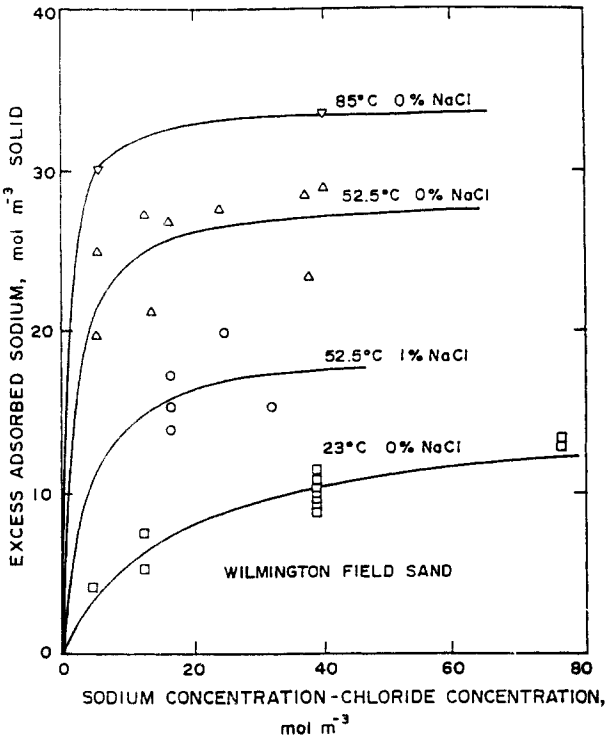


**Figure 1. Reversible sodium ion exchange isotherm.**

our form and Bunge's are equivalent. Since the medium is assumed to be water-wet, it is taken for granted that Eq. 7 holds in exactly the same form even in the presence of oil. This also means that we ignore any effect that the neutralization reaction may have on altering the empirically obtained adsorption isotherm of Eq. 7. Moreover, it is assumed that no other species including $A^-$ adsorb on the mineral surface.

The constants $K_r(C_2, T)$ and $\bar{n}_\infty(C_2, T)$ are obtained by a least square fit to Bunge's (1982) data at a given temperature and NaCl concentration. A solid specific gravity of 2.5 was used throughout. Both the least squares curves and Bunge's data are shown in Figure 1. For interpolation purposes we used

$$\bar{n}_r(C_2, T) = \bar{n}_\infty(0, T)(1 + a_{n_r} C_2), \tag{8}$$

and

$$K_r(C_2, T) = K_r(0, T)(1 + a_{C_2} C_2). \tag{9}$$

where $a_{n_r}$ and $a_{C_2}$ are constants obtained through data at 325.5 K with $C_{Cl^-} = 0$ and 1 wt. %. Only at this temperature was varying salinity data obtained by Bunge (1982). The functions $\bar{n}_\infty(0, T)$ and $K_r(0, T)$ were assumed quadratic with respect to $T$.

## Formulation of the Problem

We make the assumptions discussed below for deriving the governing conservation equations. The porous medium is presumed to be nondeformable, *ideal* (Ramakrishnan, 1985), isothermal and water-wet. We restrict ourselves to a linear, one-dimensional problem. Both oil and aqueous phases are taken to be incompressible. Given the low velocity of the fluid displacement, we assume that local equilibrium exists both for fluid-fluid and solid-fluid chemical interactions. The equilibrium constants are considered to be insensitive to pressure. We do not account for emulsions. Also, hydrodynamic dispersion and body forces are neglected. It is taken for granted that continuum hypothesis could be used. Moreover, the displacement process is considered to be stable.

Since emulsion formation is neglected, only two-phase flow need to be considered. We will use the fractional flow theory to describe the movement of the two phases where the fractional flow of a given phase is defined to be the superficial velocity of that phase divided by the total velocity. The fractional flow equations are assumed to correspond to that of a *pseudosteady displacement* process at a given capillary number. The expressions we use in this work were obtained from the relative permeability equations of Ramakrishnan and Wasan (1986). For a detailed discussion on this aspect we refer the reader to Ramakrishnan (1985). For our purpose here, it is sufficient to know that once the local capillary number is known, it is possible to obtain fractional flow of oil and water through the relative permeability equations mentioned above.

As presented earlier we shall hold the chloride ion concentration as a parameter for the problem. We will also regard that the concentration level of chemical agents such as species A and Na are low enough that both $C_{H_2O}$ and $C_o$ may be regarded as constants. The same is assumed to be true for the phase densities. Then there are three independent conservation equations. These are for hydrogen and oxygen, Na, and species A (Ramakrishnan and Wasan, 1989). Because of the diluteness of the chemical components, conserving hydrogen and oxygen is the same as conserving water and is

$$\phi \frac{\partial S_w}{\partial t} + \frac{\partial V f_w}{\partial x} = 0, \tag{10}$$

where $\phi$ is the porosity, $S_w$ is the saturation of aqueous phase, $t$ is the time, $x$ is the distance in the macroscopic flow direction, $f_w$ is the fractional flow to water (aqueous phase) and $V$ is the overall superficial velocity. A similar equation may be written for oil solvent species. This, when added to Eq. 10, leads to the conclusion that the velocity $V$ is a function of $t$ alone. For the sake of simplicity, we shall henceforth consider only the case where $V$ is kept constant. For Na conservation, in view of the small amount of acid usually encountered in crude oils, we may assume that the consumption due to the neutralization reaction is small. Thus, conserving sodium leads to

$$\phi \frac{\partial S_w C_{\mathrm{Na}^+}}{\partial t} + (1 - \phi) \frac{\partial \bar{n}_{\mathrm{Na}}}{\partial t} + \frac{\partial V f_w C_{\mathrm{Na}^+}}{\partial x} = 0. \tag{11}$$

The system chemistry as presented above implies that most of species A is present either as $HA_o$ or $NaA_o$ (Ramakrishnan and Wasan, 1983, 1989). Therefore species A conservation gives

$$\phi \frac{\partial (1 - S_w)(C_{\mathrm{HA}_o} + C_{\mathrm{NaA}_o})}{\partial t} + \frac{\partial V (1 - f_w)(C_{\mathrm{HA}_o} + C_{\mathrm{NaA}_o})}{\partial x} = 0. \tag{12}$$

We now define the normalized surfactant concentration to be

$$\delta_A = \frac{C_{HA_o} + C_{NaA_o}}{C_{(HA_o)_0}}, \tag{13}$$

and normalized sodium concentration to be

$$\beta_{Na} = \frac{C_{Na^+} - C_2}{C_{1f}}, \tag{14}$$

where $C_{1f}$ is arbitrarily fixed at 250 mol · m$^{-3}$ (=1 wt. % NaOH). Writing dimensionless time as $\tau = tV/L\phi$ where $L$ is the length of the medium and dimensionless distance $z$ as $x/L$ and using Eq. 10 to simplify Eq. 11 and 12 we get

$$\begin{pmatrix} \frac{\partial S_w}{\partial \tau} \\ \frac{\partial \delta_A}{\partial \tau} \\ \frac{\partial \beta_{Na}}{\partial \tau} \end{pmatrix} + \begin{pmatrix} \frac{\partial f_w}{\partial S_w} & \frac{\partial f_w}{\partial \delta_A} & \frac{\partial f_w}{\partial \beta_{Na}} \\ 0 & \frac{1 - f_w}{1 - S_w} & 0 \\ 0 & 0 & \frac{f_w}{S_w + \kappa \eta_{Na}} \end{pmatrix} \begin{pmatrix} \frac{\partial S_w}{\partial z} \\ \frac{\partial \delta_A}{\partial z} \\ \frac{\partial \beta_{Na}}{\partial z} \end{pmatrix} = 0. \tag{15}$$

where

$$\eta_{Na} = \frac{\zeta}{(1 + \zeta \beta_{Na})^2}, \tag{16}$$

$$\kappa = \frac{\nu \bar{n}_\infty}{C_{1f}}, \tag{17}$$

$$\zeta = K_r C_{1f}, \tag{18}$$

and

$$\nu = \frac{1 - \phi}{\phi}. \tag{19}$$

According to the interfacial activity model presented by Ramakrishnan and Wasan (1983), only species $A^-$ adsorbs in significant quantity at the water-oil interface. The resulting reduction in interfacial tension is determined by $C_{A^-}$ and $C_e$, the electrolyte concentration. From the equilibrium chemistry these are

$$C_{A^-} = \frac{C_{(HA_o)_0} \delta_A}{\left[ \frac{2K_D K_w}{K_A [C_{1f} \beta_{Na} + \sqrt{C_{1f}^2 \beta_{Na}^2 + 4K_w}]} + \frac{C_{1f} \beta_{Na} + \xi_{Na} C_{2f}}{K_s} \right]}, \tag{20}$$

and

$$C_e = \xi_{Na} C_{2f} + \tfrac{1}{2}[C_{1f} \beta_{Na} + \sqrt{C_{1f}^2 \beta_{Na}^2 + 4K_w}], \tag{21}$$

where

$$\xi_{Na} = \frac{C_2}{C_{2f}}. \tag{22}$$

$C_2$ is the injection concentration of NaCl and is equal to $C_{Cl^-}$ and will be held as a parameter. $C_{2f}$ is a reference concentration fixed at 1 wt. % NaCl or 171.11 mol · m$^{-3}$.

Knowing $C_{A^-}$ and $C_e$, the interfacial tension is evaluated from a set of coupled equations. These equations arise from the adsorption isotherm and equation of state for the surface (Ramakrishnan and Wasan, 1983) and are:

$$C_{A^-} = \frac{k_2}{k_1} \frac{n_{A^-}}{\left(1 - \frac{n_{A^-}}{n_{max}}\right)} \exp\left\{\frac{-[W + N\epsilon\psi(0)]}{RT}\right\}, \tag{23}$$

where

$k_1$ = adsorption rate constant
$k_2$ = desorption rate constant
$n_{A^-}$ = moles of $A^-$ per unit area at the interface
$n_{max}$ = maximum number of moles that can be adsorbed per unit area of the interface
$W$ = energy barrier for desorption
$N$ = Avagadro number
$\epsilon$ = electronic charge
$\psi(0)$ = sublayer potential
$R$ = gas constant

The sublayer potential is (all equations with permittivity are presented in SI units):

$$\psi(0) = \frac{-2kT}{\epsilon} \sinh^{-1}\left[\frac{(n_{A^-})\epsilon N^{1/2}}{2^{3/2}(\epsilon_r \epsilon_0)^{1/2}(kT)^{1/2} C_e^{1/2}}\right], \tag{24}$$

where

$k$ = Boltzmann constant
$\epsilon_r$ = relative permittivity of the medium
$\epsilon_0$ = permittivity of vacuum

To calculate interfacial tension $\gamma$, we use the interface equation of state which is

$$\gamma - \gamma_0 = RTn_{max} \ln\left(\frac{1}{1 - n_{A^-}/n_{max}}\right) + \frac{4\sqrt{2}}{\epsilon}(kT)^{3/2}(N\epsilon_r\epsilon_0 C_e)^{1/2}\left[\cosh\frac{\epsilon\psi(0)}{2k_B T} - 1\right], \tag{25}$$

where $\gamma_0$ is the "clean" water-oil interfacial tension. Thus, once the concentrations $\delta_A$ and $\beta_{Na}$ are known using Eq. 20 to 25, we may calculate oil-water interfacial tension. This can then be used to simultaneously calculate a unique value of both the capillary number and the fractional flow for a given overall superficial velocity $V$ and saturation (for details see Ramakrishnan, 1985).

To complete the formulation we now specify the initial conditions. We shall call the initial condition for $z < 0$ as the *injection state*. This is given by

$$\begin{pmatrix} S_w \\ \delta_A \\ \beta_{Na} \end{pmatrix} = \begin{pmatrix} 1 \\ 0 \\ \beta_{Na}^0 \end{pmatrix}, \tag{26}$$

where $\beta^0_{Na} = C_1/C_{1f}$ and $C_1$ is the injection concentration of NaOH. The *initial state* is the initial condition for $z > 0$ and is

$$\begin{pmatrix} S_w \\ \delta_A \\ \beta_{Na} \end{pmatrix} = \begin{pmatrix} S_{rw} \\ 1 \\ 0 \end{pmatrix}, \tag{27}$$

for secondary stimulated recovery, where an alkaline solution is injected into a predominantly oil filled medium, and

$$\begin{pmatrix} S_w \\ \delta_A \\ \beta_{Na} \end{pmatrix} = \begin{pmatrix} 1 - S^0_{ro,m} \\ 1 \\ 0 \end{pmatrix}. \tag{28}$$

for tertiary recovery, where the alkali is injected following several pore volumes of brine injection (waterflood). In the above equations $S_{rw}$ is the residual water saturation and $S^0_{ro,m}$ is the maximum residual oil saturation which is the same as the waterflood residual oil saturation starting from an initial condition corresponding to Eq. 27.

The problem posed by the differential equation system (Eq. 15), along with Eqs. 16 to 25, the initial conditions, and the fractional flow equations constitute a Riemann problem (for recent discussions on this subject, refer to Dafermos, 1983; Ramakrishnan, 1985). The Riemann problem possesses solutions which are functions of $z/\tau$ alone and may be solved by the method of generalized Riemann invariants. This method is discussed in detail in the above-mentioned references. The following sections therefore presume that the reader is familiar with this method and the earlier results of the problem where adsorption effects on the solid surface were not included.

## Analytical and Numerical Results

The coefficient matrix in Eq. 15 is now denoted $A(u)$. $u$ is the column vector of dependent variable elements which are $S_w$, $\delta_A$ and $\beta_{Na}$. The eigenvalues of $A$ are

$$\lambda^{(p)} = \frac{\partial f_w}{\partial S_w}, \tag{29}$$

$$\lambda^{(q)} = \frac{1 - f_w}{1 - S_w}, \tag{30}$$

and

$$\lambda^{(r)} = \frac{f_w}{S_w + \kappa\eta_{Na}}. \tag{31}$$

Superscripts $p$, $q$ and $r$ are meant to indicate a particular eigenvalue and may take on values from one to three where the smallest index denotes the smallest eigenvalue. The corresponding right eigenvectors $(dS_w, d\delta_A, d\beta_{Na})^T$ of the $p$, $q$ and $r$ family are

$$r^{(p)} = dl \begin{pmatrix} 1 \\ 0 \\ 0 \end{pmatrix}, \tag{32}$$

$$r^{(q)} = dl \begin{pmatrix} \dfrac{\partial f_w}{\partial \delta_A} \\ \dfrac{1 - f_w}{1 - S_w} - \dfrac{\partial f_w}{\partial S_w} \\ 0 \end{pmatrix}, \tag{33}$$

and

$$r^{(r)} = dl \begin{pmatrix} \dfrac{\partial f_w}{\partial \beta_{Na}} \\ 0 \\ \dfrac{f_w}{S_w + \kappa\eta_{Na}} - \dfrac{\partial f_w}{\partial S_w} \end{pmatrix}, \tag{34}$$

where $l$ is an arbitrary parameter. The right eigenvectors, when integrated, give rise to the *simple wave curves* of the three families and for convenience are denoted $\Gamma^{(k)}$. $k$ is assigned a value from one to three depending on the magnitude of the eigenvalue associated with the simple wave curve at the point of interest in the dependent variable space (a larger number implies a higher eigenvalue). Analogous to the nomenclature for eigenvalues and eigenvectors we also use the indices of $p$, $q$ and $r$ to denote the simple wave curves associated with a particular family.

The differential form for the simple wave curves given by Eqs. 32 to 34 implies that no more than two dependent variables can change along a simple wave curve. Moreover, one of the two variables is $S_w$. Therefore, we analyze $(P, Q)$ and $(P, R)$ composition planes independently. The $(P, Q)$ planes consist of $p$ and $q$ simple wave curves at a fixed $\beta_{Na}$. The $(P, R)$ planes consist of $p$ and $r$ simple wave curves at a fixed $\delta_A$.

Discontinuity curves for the three families are obtained by satisfying the Rankine-Hugoniot conditions (Jeffery, 1976). These are

$$\Lambda^{(p)} = \frac{f^p_w - f^m_w}{S^p_w - S^m_w}; \quad \beta^p_{Na} = \beta^m_{Na}; \quad \delta^p_A = \delta^m_A, \tag{35}$$

$$\Lambda^{(q)} = \frac{f^p_w - f^m_w}{S^p_w - S^m_w} = \frac{(1 - f^p_w)\delta^p_A - (1 - f^m_w)\delta^m_A}{(1 - S^p_w)\delta^p_A - (1 - S^m_w)\delta^m_A}$$

$$= \frac{1 - f^p_w}{1 - S^p_w} = \frac{1 - f^m_w}{1 - S^m_w}; \quad \beta^p_{Na} = \beta^m_{Na}, \tag{36}$$

and

$$\Lambda^{(r)} = \frac{f^p_w - f^m_w}{S^p_w - S^m_w} = \frac{f^p_w\beta^p_{Na} - f^m_w\beta^m_{Na}}{S^p_w\beta^p_{Na} - S^m_w\beta^m_{Na} + \dfrac{\kappa\zeta(\beta^p_{Na} - \beta^m_{Na})}{(1 + \zeta\beta^p_{Na})(1 + \zeta\beta^m_{Na})}}$$

$$= \frac{f^p_w}{S^p_w + \dfrac{\kappa\zeta}{(1 + \zeta\beta^p_{Na})(1 + \zeta\beta^m_{Na})}} = \frac{f^m_w}{S^m_w + \dfrac{\kappa\zeta}{(1 + \zeta\beta^p_{Na})(1 + \zeta\beta^m_{Na})}};$$

$$\delta^p_A = \delta^m_A. \tag{37}$$

Here superscripts $p$ and $m$ stand for plus and minus sides of the discontinuity. By convention, the plus side is the one toward

which the discontinuity propagates. The last result in Eq. 37 is different from the inert solid model, because $\Lambda^{(r)}$ is modified to account for Na adsorption. This is what gives rise to the interesting mathematical properties of system 15.

### *Simple wave curves*

The values of the parameters held constant for all computations were those of Long Beach crude (Ramakrishnan and Wasan, 1983). Thus, $K_A/K_D = 5 \times 10^{-12}$ mol · m$^{-3}$, $K_s = 0.175$ mol · m$^{-3}$, $W \equiv 13$ $CH_2$ groups, $C_{(HA_o)_0} = 34.875$ mol · m$^{-3}$, $\gamma_0 = 31.6$ mol · m$^{-1}$, and $T = 298$ K. The residual water saturation was 0.1. The waterflood residual oil saturation was kept at 0.3. Fixing a value of $C_2$ or $\xi_{Na}$ also fixes the parameters $\kappa$ and $\zeta$ through Eq. 8 and 9. Rather than using $\kappa$ and $\zeta$ as independent parameters, we employ the interpolated data of Bunge and Radke (1982) on Wilmington field sand in all our computations. For $\nu$, we used a value of 4 which is equivalent to a $\phi$ of 0.2. The numerical procedure for computing simple wave curves is the same as that in Ramakrishnan and Wasan (1989).

As anticipated, no essential differences were observed in the $(P, Q)$ composition plane at a $\beta_{Na} = 1$, when ion exchange was included. Thus, the $p$-field is a line field and the $q$-field is exceptional (Liu, 1974). As we already know, the $(P, Q)$ composition plane permits us to introduce a zero velocity discontinuity in $\delta_A$ from 0 to 1 at an aqueous-phase saturation of one. This can then be combined with a zero velocity $p$-discontinuity. The extent of this discontinuity is dependent on the $(P, R)$ composition plane which we now proceed to discuss.

From the earlier work (Ramakrishnan and Wasan, 1989), we known that the relevant plane for the deduction of *composition route* is the $(P, R)$ composition plane at a $\delta_A = 1$. This plane is shown in Figure 2. In this figure, arrows show the direction of increasing eigenvalue for the corresponding field, whereas a sinusoidal notation on the simple wave curve implies that the eigenvalue is a constant as one proceeds along the wave curve. A circle on the sinusoidal notation indicates that the constant value is zero. The composition route consists of wave curves which connect state $\boldsymbol{u}^{(0')}$ to either $\boldsymbol{u}_s^+$ (secondary recovery) or $\boldsymbol{u}_t^+$ (tertiary recovery) as the case may be. The state $\boldsymbol{u}^{(0')}$ itself is connected by zero velocity discontinuity to the injection state in the $(P, Q)$ plane as stated above. The upright and the inverted U structures of the $r$-simple wave curves are retained in the presence of adsorption due to the under-optimum $[(\partial f_w)/(\partial \beta_{Na}) < 0]$ and over-optimum $[(\partial f_w)/(\partial \beta_{Na}) > 0]$ regions. Wherever the $r$-simple wave curves are vertical, $(\partial f_w)/(\partial \beta_{Na}) = 0$ (the optimal region), and wherever $p$- and $r$-simple wave curves are tangential, $\lambda^{(p)}$ is equal to $\lambda^{(r)}$.

In spite of the close similarity between these $r$-simple wave curves and those of the previous work of Ramakrishnan and Wasan (1989) (shown in Figure 3) we note some drastic changes in the neighborhood of the curve on which $\lambda^{(p)} = \lambda^{(r)}$ as well as $(\partial f_w)/(\partial \beta_{Na}) = 0$. A numerical solution on this curve using Eq. 34 is meaningless because $\boldsymbol{r}^{(r)}$ is identically zero. However, we can resort to the original partial differential equations to deduce the acceptable simple wave curves. This shows that in the region where $[(\partial f_w)/(\partial \beta_{Na})] = 0$, not only are vertical lines (constant $S_w$) acceptable, but also the curve along which $\lambda^{(p)} = \lambda^{(r)}$. Below the $\lambda^{(p)} = \lambda^{(r)}$ curve the vertical lines are $\Gamma^{(2)}$, whereas above the $\lambda^{(p)} = \lambda^{(r)}$ curve they become $\Gamma^{(3)}$. One such vertical line is shown in Figure 2 for illustration. Analogous to the case of zero adsorption, we have also marked upper and lower critical points.

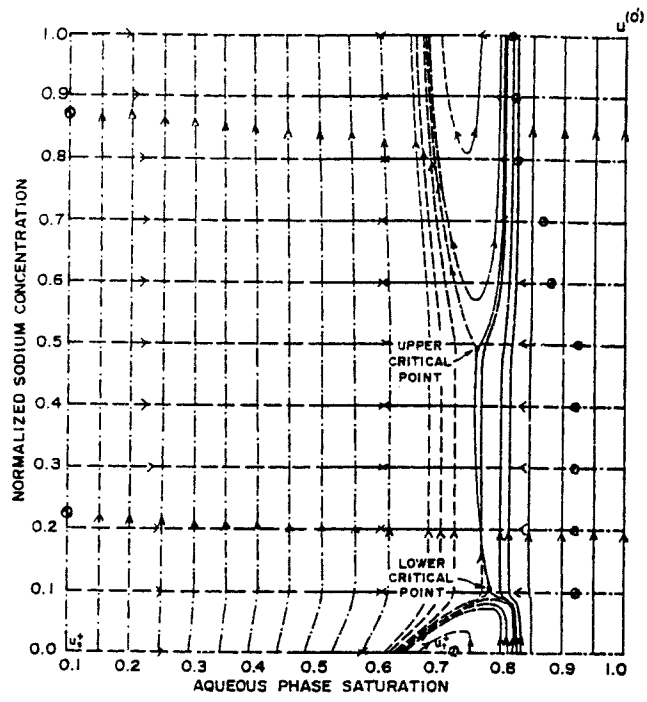


**Figure 2. $(P, R)$ composition plane with reversible ion exchange.**

——— $\Gamma^{(3)}$, - - - $\Gamma^{(2)}$, ——— $\Gamma^{(1)}$

$\bar{N}_{c0} = 4 \times 10^{-7}$, $M_\mu = 1$, $\delta_A = 1$, $\xi_{Na} = 1$

From the $(P, R)$ composition plane it is evident that a dilemma arises in the contruction of the compostion route. In proceeding from state $\boldsymbol{u}^{(0')}$ we see that an infinite number of simple wave curves exist to reach $\beta_{Na} = 0$ from a $\beta_{Na} = 1$ ($\beta^0_{Na} = 1$ is taken as an example). Each vertical line crossing the $\lambda^{(p)} = \lambda^{(r)}$ curve gives rise to a different simple wave curve with different states $\boldsymbol{u}^{(1)}$ and $\boldsymbol{u}^{(2)}$ where $\boldsymbol{u}^{(1)}$ and $\boldsymbol{u}^{(2)}$ are the intersection point of the selected $\Gamma^{(r)}$ curve with the lines $\beta_{Na} = 1$ and $\beta_{Na} = 0$, respectively (see Figure 3). Furthermore, the $\lambda^{(p)} = \lambda^{(r)}$ curve can also be used.

A closer examination of $r$-simple wave curves resolves the dilemma of composition route construction at least temporarily. Unlike the case of zero adsorption where it was found that the $r$-field was exceptional, Figure 2 shows that $\lambda^{(r)}$ increases wherever $\beta_{Na}$ increases along a simple curve. Accepting this numerical result momentarily and using Liu's (1974) condition as the basis, it is readily seen that an $r$-simple wave construction fails for states on the left (toward injection state) having a higher $\beta_{Na}$ than those on the right (toward initial state). For such cases, we know that discontinuity curves have to be used to obtain the composition route. It is, however, unclear whether a unique solution would result from an analysis of discontinuity curves.

The numerical result that $\lambda^{(r)}$ increases whenever $\beta_{Na}$ increases along an $r$-simple wave curve can be verified analytically through Eq. 31. Taking the total differential we get

$$d\lambda^{(r)} = \frac{1}{S_w + \kappa\eta_{Na}} \left\{ [\lambda^{(p)} - \lambda^{(r)}]\, dS_w + \frac{\partial f_w}{\partial \beta_{Na}}\, d\beta_{Na} - \lambda^{(r)} \kappa \eta'_{Na}\, d\beta_{Na} \right\} \quad (38)$$

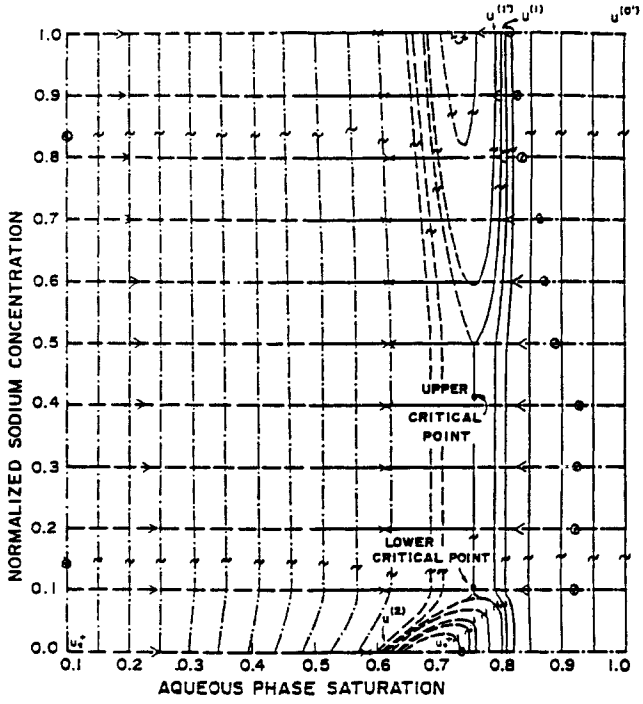


**Figure 3. (P, R) composition plane with no ion exchange.**
$\Gamma^{(3)}$, $\Gamma^{(2)}$, $\Gamma^{(1)}$
$\bar{N}_{c0} = 4 \times 10^{-7}$, $M_\mu = 1$, $\delta_A = 1$, $\xi_{Na} = 1$

Whenever Eq. 34 is valid, the first two terms in Eq. 38 cancel each other. When Eq. 34 is not meaningful $\lambda^{(p)} = \lambda^{(r)}$ and $(\partial f_w)/(\partial \beta_{Na}) = 0$. Hence for either case

$$d\lambda^{(r)} = -\lambda^{(r)} \kappa \eta'_{Na}\, d\beta_{Na}. \tag{39}$$

Since $\lambda^{(r)} > 0$, $\kappa > 0$, $\eta'_{Na} < 0$, we have the result that along an $r$-simple wave curve $d\lambda^{(r)} > 0$, whenever $d\beta_{Na} > 0$; or $\lambda^{(r)}$ is a monotonically increasing function of $\beta_{Na}$ along an $r$-simple wave curve. Thus, based on this result, a continuous solution in which the Na concentration varies is impossible. Only discontinuities are acceptable. Moreover, these discontinuities are not exceptional, i.e., they will be sustained in spite of dispersion.

### r-discontinuity wave curves

The $r$-discontinuity curves in the $(P, R)$ composition plane obey Eq. 37. Unlike the simple wave curves, they change with the fixed state at which the parameter $l$ along a discontinuity curve is equal to zero. Since we know that the initial state has a $\beta_{Na} = 0$, let us attempt at generating only those $r$-discontinuity curves which have fixed states on the $\beta_{Na} = 0$ axis. With $\beta^p_{Na} = 0$, Eq. 37 can be expressed as

$$\Lambda^{(r)} = \frac{f^p_w - f^m_w}{S^p_w - S^m_w} = \frac{f^p_w}{S^p_w + \dfrac{\kappa\zeta}{1 + \zeta\beta^m_{Na}}}. \tag{40}$$

Since the state $p$ is kept fixed and the aim is to obtain the discontinuity curve by finding states $m$ that satisfy Eq. 40, the superscripts $m$ and $p$ are removed. We denote the fixed state $S^p_w$ as $S$ and $f^p_w$ as $F$. Thus,

$$\Lambda^{(r)} = \frac{f_w - F}{S_w - S} = \frac{F}{S + \dfrac{\kappa\zeta}{1 + \zeta\beta_{Na}}}. \tag{41}$$

Given an $S$, $F$ is known and therefore Eq. 41 is a relationship between $S_w$ and $\beta_{Na}$. This should yield a curve in the $(P, R)$ composition plane. The difficulty in directly obtaining the discontinuity curve is that given a $\beta_{Na}$ multiple roots of $S_w$ are possible for Eq. 41. Moreover, for certain $\beta_{Na}$'s a root may not exist for $S_w$. To deal with such cases it is instructive to derive a differential equation for $\beta_{Na}$ from Eq. 41.

Differentiating Eq. 41 with respect to $S_w$ gives

$$\frac{df_w}{dS_w}\left[S + \frac{\kappa\zeta}{1 + \zeta\beta_{Na}}\right] + \left[\frac{d}{dS_w}\left(\frac{\kappa\zeta}{1 + \zeta\beta_{Na}}\right)\right](f_w - F) = F. \tag{42}$$

Utilizing the chain rule

$$\frac{df_w}{dS_w} = \frac{\partial f_w}{\partial S_w} + \frac{\partial f_w}{\partial \beta_{Na}}\frac{d\beta_{Na}}{dS_w}, \tag{43}$$

in the $(P, R)$ composition plane, Eq. 42 yields

$$\frac{d\beta_{Na}}{dS_w} = \frac{\Lambda^{(r)} - \lambda^{(p)}}{\dfrac{\partial f_w}{\partial \beta_{Na}} + \kappa\left(\dfrac{\zeta}{1 + \zeta\beta_{Na}}\right)^2 [\Lambda^{(r)} - \bar{\lambda}^{(r)}]}, \tag{44}$$

where

$$\bar{\lambda}^{(r)} = \frac{f_w}{S + \dfrac{\kappa\zeta}{1 + \zeta\beta_{Na}}}. \tag{45}$$

Equation 44 is very similar to the differential equation for the $r$-simple wave curve given by Eq. 34. However, for discontinuity curves, even when $(\partial f_w)/(\partial \beta_{Na}) = 0$, $dS_w$ may be nonzero due to the second term in the denominator. Indeed, it is this term which causes the deviation of the discontinuity curve from the simple wave curve. This is expected in view of the fact that the $r$-characteristic field is neither an exceptional field nor a line field (Temple, 1983).

The numerical technique for generating the discontinuity curve is to integrate Eq. 44 from $\beta_{Na} = 0, S_w = S$ (for details see Ramakrishnan, 1985). However, it was usually found that after a few steps of integration the discontinuity relation (Eq. 41) itself was not satisfied accurately. In view of this, after a sufficient number of steps it is necessary to use the integrated solution as a starting guess and an $S_w$ for the given $\beta_{Na}$ that satisfies Eq. 41 has to be iterated for. The algorithm used for this purpose is written so that there would be little difficulty when there is a double root. As indicated by the differential form of the discontinuity curve, double roots occur if $\Lambda^{(r)} = \lambda^{(p)}$ for some

value of $S_w$, provided:

$$\frac{\partial f_w}{\partial \beta_{Na}} + \kappa \left(\frac{\zeta}{1 + \zeta \beta_{Na}}\right)^2 [\Lambda^{(r)} - \bar{\lambda}^{(r)}] \neq 0.$$

At such points, the $r$-discontinuity curve becomes tangential to the $p$-wave curve. If no $S_w$ satisfying Eq. 41 is found, the value of the numerically integrated $\beta_{Na}$ is reduced and the proper value of $S_w$ satisfying Eq. 41 is found.

The point, where the numerator and the denominator of Eq. 44 become zero, is the *critical point* for the autonomous system

$$\frac{d\beta_{Na}}{dl} = \Lambda^{(r)} - \lambda^{(p)}, \tag{46}$$

and

$$\frac{dS_w}{dl} = \frac{\partial f_w}{\partial \beta_{Na}} + \kappa \left(\frac{\zeta}{1 + \zeta \beta_{Na}}\right)^2 [\Lambda^{(r)} - \bar{\lambda}^{(r)}], \tag{47}$$

and is reached only when $l \rightarrow \infty$. Therefore, to obtain the critical point the system

$$\Lambda^{(r)} - \lambda^{(p)} = 0, \tag{48}$$

$$\frac{\partial f_w}{\partial \beta_{Na}} + \kappa \left(\frac{\zeta}{1 + \zeta \beta_{Na}}\right)^2 [\Lambda^{(r)} - \lambda^{(p)}] = 0, \tag{49}$$

and Eq. 41 has to be simultaneously solved. This gives the three unknowns $\beta_{Na}$ and $S_w$ at the critical point and the saturation $S$. The complete discontinuity curves passing through the critical point are obtained by starting from the critical point, making small changes in $\beta_{Na}$ and $S_w$, satisfying Eq. 41 and proceeding with the method discussed earlier for obtaining the discontinuity curves. Four different curves starting from the critical point with $S = S^c$ can be obtained. As an example, consider a small increase in both $\beta_{Na}$ and $S_w$. Doing so would make:

$$\Lambda^{(r)} > \lambda^{(p)}$$

and

$$\frac{\partial f_w}{\partial \beta_{Na}} + \kappa \left(\frac{\zeta}{1 + \zeta \beta_{Na}}\right)^2 [\Lambda^{(r)} - \bar{\lambda}^{(r)}] > 0.$$

Integrating from this point, Eq. 44 would continue to increase both $\beta_{Na}$ and $S_w$ at least for a small neighborhood of the critical point. Similarly decreasing both $\beta_{Na}$ and $S_w$ would cause $\Lambda^{(r)}$ to be less than $\lambda^{(p)}$ and

$$\frac{\partial f_w}{\partial \beta_{Na}} + \kappa \left(\frac{\zeta}{1 + \zeta \beta_{Na}}\right)^2 [\Lambda^{(r)} - \lambda^{(p)}]$$

to be less than zero so that numerical integration causes both $\beta_{Na}$ and $S_w$ to decrease. For this curve $S_w$ at $\beta_{Na} = 0$ is denoted $S^c$. By reversing the signs of both the numerator and the denominator in Eq. 44, two more discontinuity curves can be constructed.

Figure 4 shows the $(P, R)$ composition plane in which $r$-simple wave curves have been replaced by $r$-discontinuity

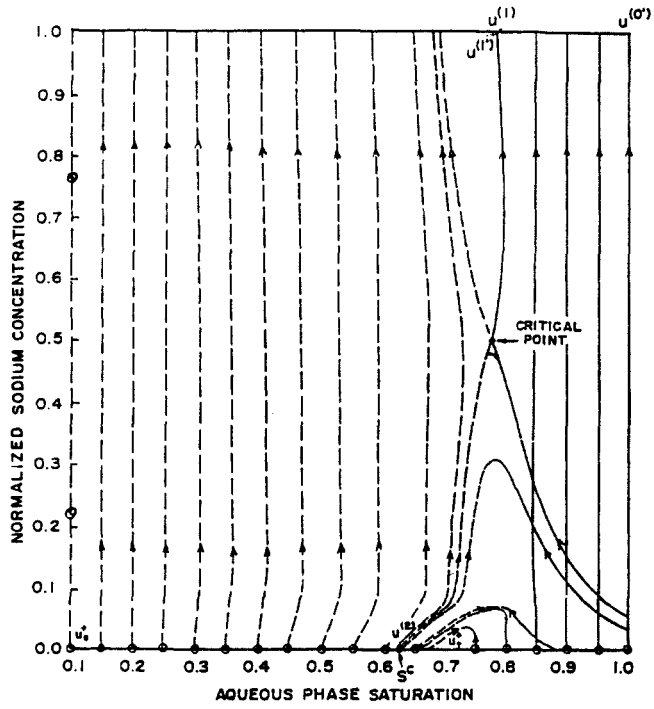


**Figure 4. $r$-discontinuity curves at 1 wt. % NaCl.**

——— $\Lambda^{(r)} > \lambda^{(q)}$, – – – $\Lambda^{(r)} < \lambda^{(p)}$

$\bar{N}_{c0} = 4 \times 10^{-7}$, $M_\mu = 1$, $\delta_A = 1$, $\xi_{Na} = 1$

curves. Only the two relevant $p$-wave curves, one at $\beta_{Na} = 0$ and the second at $\beta_{Na} = 1$ are shown. These are drawn as solid lines, whereas the $r$-discontinuity curves are marked as dashed or solid lines depending on whether $\Lambda^{(r)} < \lambda^{(p)}$ or $\Lambda^{(r)} > \lambda^{(p)}$. This is sufficient to identify possible composition routes. Since the discontinuity curves depend on the fixed state, fixed states are marked with circles around them. Evidently, only those curves originating from $\beta_{Na} = 0$ are shown.

Based on numerical computations, the arrows on the $r$-discontinuity curves show the direction of increasing $\Lambda^{(r)}$. When $F = 0$, the value of $\Lambda^{(r)}$ remains zero. From Figure 4 it is clear that $\Lambda^{(r)}$ monotonically increases with $\beta_{Na}$. This can be verified by deriving the total differential of $\Lambda^{(r)}$ from

$$\Lambda^{(r)} = \frac{F}{S + \dfrac{\kappa\zeta}{1 + \zeta\beta_{Na}}}, \tag{50}$$

along the $r$-discontinuity curve. This is

$$d\Lambda^{(r)} = \frac{F\kappa\zeta^2\, d\beta_{Na}}{[S(1 + \zeta\beta_{Na}) + \kappa\zeta]^2}. \tag{51}$$

It is obvious from Eq. 51 that $d\Lambda^{(r)} > 0$, if $d\beta_{Na} > 0$. Liu's (1974) condition for admissible discontinuities can now be applied. Let us suppose that $l$ is the negative arc length along $r$-discontinuity curve. Say $l = l^p = 0$ at $\beta_{Na} = \beta^p_{Na}$ and $l = l^m$ at $\beta_{Na} = \beta^m_{Na}$. As mentioned earlier, superscripts $p$ and $m$ refer to the plus (downstream) and minus (upstream) states, respectively. From Liu's condition and Eq. 51, we arrive at the important conclu-

sion that for an $r$-discontinuity to be admissible

$$\beta^m_{Na} = \beta_{Na}(l = l^m) \geq \beta_{Na}(l), \quad l^m \leq l \leq 0, \qquad (52)$$

that is, the upstream sodium concentration will be higher than the downstream value.

### *Composition route*

The sequence of wave curves forming the composition route is apparent now. In principle, the main difference from the case of no adsorption is the $r$-wave curve. To recap, in the $(P, R)$ plane which is used following the jump to state $u^{(0)}$ from $u^-$ in the $(P, Q)$ plane, we proceed on the zero velocity $p$-wave curve. This $p$-discontinuity has a $\Lambda = 0$ and is traced on the $\beta_{Na} = \beta^0_{Na}$ line. For the purpose of the discussion, it is assumed that $\beta^0_{Na} = 1$.

The zero velocity $p$-wave curve is used until either $u^{(1)}$ or $u^{(1')}$ is reached, depending on which one of the two states has a larger $S_w$. $u^{(1)}$ is the point where the $p$-wave curve of $\beta_{Na} = 1$ and the $r$-wave curve *through the critical point* intersect. The point $u^{(1')}$ on $\beta_{Na} = 1$ is where $\lambda^{(p)}$ just becomes zero as we increase $S_w$ from $S_{rw}$. In Figure 4 the point $u^{(1')}$ has a $S_w$ which is slightly less than that of $u^{(1)}$. In such cases, the nonzero velocity $p$-wave curve is absent and we switch to the $r$-wave curve at $u^{(1)}$. If $u^{(1)}$ had a smaller $S_w$ than at $u^{(1')}$ we would have constructed a $p$-wave curve with $\lambda^{(p)} > 0$ until we reached $u^{(1)}$ and then switched to the $r$-wave curve. This, for example, is the situation for a $\xi_{Na} = 0.5$ and $\beta^0_{Na} = 1$ (see Figure 5). The curves are similar to the $\xi_{Na} = 1$ case, except that a $p$-wave (simple wave) curve with $\lambda^{(p)} > 0$ is present between $u^{(1)}$ and $u^{(1')}$.

For both of the cases discussed above, from the $p$-wave curve at $u^{(1)}$ the $r$-wave (discontinuity) curve passing through the critical point is taken. This has a $\Lambda^{(r)} > \lambda^{(p)}$ at $u^{(1)}$ and therefore the change from one wave curve to another does not create uniqueness problems. Similarly, at $u^{(2)}$ where the $r$-wave curve intersects the $\beta_{Na} = 0$ $p$-wave curve, $\Lambda^{(r)} < \lambda^{(p)}$. However, since the final segment of the composition route always turned out to be a $p$-discontinuity, the more relevant condition is that $\Lambda^{(r)} \leq \Lambda^{(p)}$ either from $u^{(2)}$ to $u_s^+$ or $u_t^+$ as the case may be. This was always found to be true.

The importance of the critical point in the $(P, R)$ composition plane is evident now. The apparent nonuniqueness shown by the simple wave curves in the composition plane is resolved by having a single critical point in the case of discontinuity curves. The only acceptable $r$-wave curve from a $\beta_{Na} = \beta^0_{Na}$ to a $\beta_{Na} = 0$ passes through the critical point as long as $\beta^0_{Na} \geq \beta_{Na}$ at the critical point. If this is not the case, from condition 52 and uniqueness requirements, it is obvious that the permissible $r$-wave curve is one which becomes tangential to the $p$-wave curve of $\beta_{Na} = \beta^0_{Na}$. *Thus, whatever be the values of $\beta^0_{Na}$ short-cut numerical procedures are possible whereby the identification of the critical point alone yields sufficient information about the r-wave curve of interest. Extensive mapping of the discontinuity curves throughout the (P, R) has been shown to be unnecessary.*

Knowing the composition route, the wave fans are easily drawn in the $(z, \tau)$ plane. Corresponding to each composition along a simple wave curve of the composition route, a line of slope $\lambda^{(k)}$ is drawn from the origin. This represents the composition velocity. For discontinuities, the wave-fan diagram is simply a line of slope $\Lambda^{(k)}$ for the origin. With the combination of both the wave fans and the composition route, the construction of solutions both in terms of history and profile is straight forward. Unfortunately, unlike the zero adsorption case, *no simple graphical procedure* seems evident when $\beta^0_{Na} > \beta_{Na}$ at the critical point. If $\beta^0_{Na}$ is less than this value, the familiar tangent construction as outlined by Pope (1980) for polymer and low concentration surfactant flooding can be used.

### *Parametric study*

Before we proceed to discuss the profiles and histories, let us first examine the effect of adsorption on the oil recovery process. For this purpose, the $(P, R)$ composition planes in Figures 3 and 4 which employ the same parameters $\bar{N}_{c0}$, $M_\mu$, and $\xi_{Na}$ are useful.

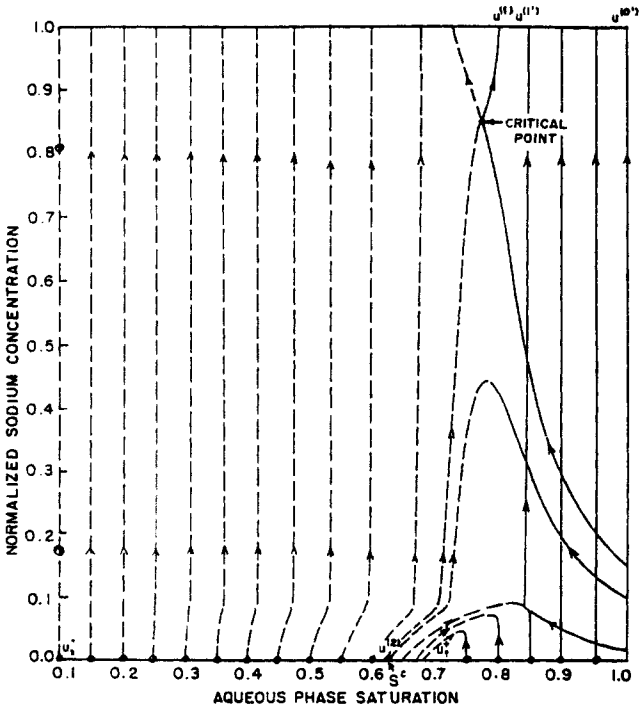


**Figure 5. $r$-discontinuity curves at 0.5 wt. % NaCl.**
——— $\Lambda^{(r)} > \lambda^{(p)}$, - - - $\Lambda^{(r)} < \lambda^{(p)}$
$\bar{N}_{c0} = 4 \times 10^{-7}$, $M_\mu = 1$, $\delta_A = 1$, $\xi_{Na} = 0.5$

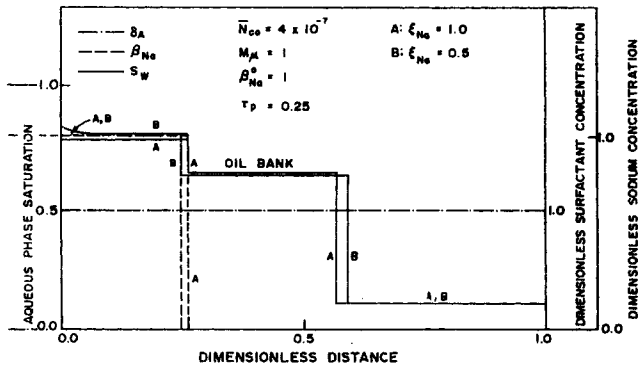


**Figure 6. Dependence of secondary recovery profiles on $C_{NaCl}$.**

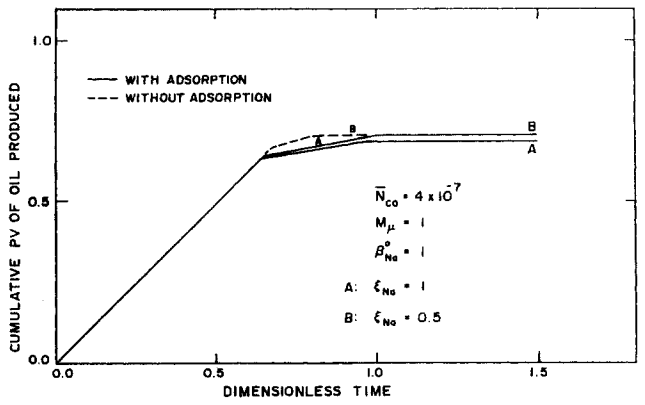


**Figure 7. Secondary recovery cumulative oil production at different $C_{NaCl}$.**

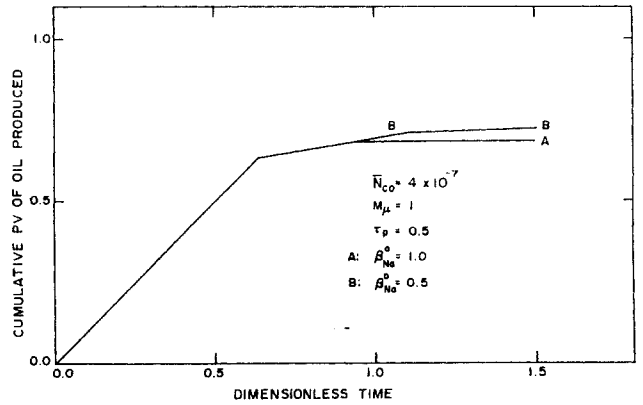


**Figure 9. Secondary recovery cumulative oil production at different injection NaOH concentrations.**

The infleunce of adsorption is evident from the predicted ultimate oil recovery. Comparing Figures 3 and 4 it is obvious that adsorption can play a detrimental role. The well separated $u^{(1)}$ and $u^{(1')}$ in Figure 3 are almost coincident in Figure 4. Note that $u^{(1')}$ remains the same in the two figures and that the composition route switches to the $r$-wave curve at $u^{(1)}$ itself. Thus, by decreasing the value of $S_w$ at $u^{(1)}$ adsorption *reduces the ultimate oil recovery.* This result is different from what is commonly perceived to be the effect of reversible adsorption when a constant composition solution is *continuously injected*—namely delayed and less efficient oil production. Apparently, the reduction in the ultimate oil recovery is caused by the increased chemical front movement rate with increaisng $\beta^0_{Na}$ values, which in turn reduces the influence of the otpimum region in determining oil removal from the medium.

The data of Bunge (1982) show that if the NaCl concentration of the system is reduced the adsorbed Na is increased. This would be reflected by a delay in the chemical front movement for a decreased NaCl concentration. Such a situation is illustrated in the secondary recovery profile plot of Figure 6.

Reduction in salt concentration and the resulting lag may not, however, cause a less efficient oil recovery process. This is because a reduced salt concentration moves the injected NaOH concentration closer to the optimum region (compare Figures 4 and 5) or in turn to the critical point. Indeed, this may reduce the detrimental effect of adsorption. To show this, we have plotted the cumulative pore volumes (PV) of oil production curves with and without adsorption for two different salinities of $\xi_{Na} = 1.0$ and 0.5 in Figure 7. When there is no adsorption, there is virtually no effect of reducing $\xi_{Na}$, because in both cases the optimum region plays a dominant role in recovering oil. When reversible ion exchange takes place, however, the increased role played by the injection composition (due to the reduced influence of the optimal region) in determining recovery reduces the ultimate amount of oil displaced. This reduction is significant for $\xi_{Na} = 1$ because the injection composition here is far away from the critical point.

The same features as in the varying salinity case are also seen when we change $\beta^0_{Na}$ from 1 ot 0.5 (see Figure 8 and 9). Here the sodium front at a $\beta^0_{Na} = 0.5$ lags behind slightly. Nevertheless, since a $\beta^0_{Na} = 0.5$ is nearly coincident with the critical point, oil continues to be swept behind the chemical front. Because the state $u^{(2)}$ is the same for any $\beta^0_{Na}$ as long as it is above the critical $\beta_{Na}$, the frontal saturation discontinuity from $u^{(2)}$ to $u_s^+$ propagates at the same velocity for $\beta_{Na}$'s = 1.0 and 0.5.

The tertiary recovery profiles and histories for varying NaCl concentrations are shown in Figures 10 and 11, respectively. As expected, the conclusions reached earlier through secondary recovery calculations are seen to be valid here. The prediction that a $\xi_{Na} = 0.5$ recovers oil more effectively can be arrived at by studying the oil bank. For a $\xi_{Na} = 0.5$, the oil bank not only produces oil more rapidly, but it also propagates faster and ends

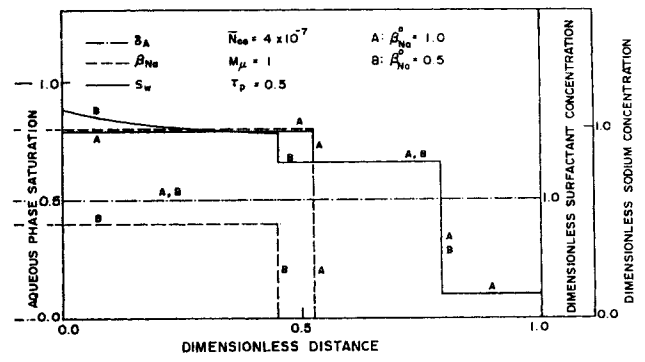


**Figure 8. Secondary recovery profiles at different injection NaOH concentrations.**

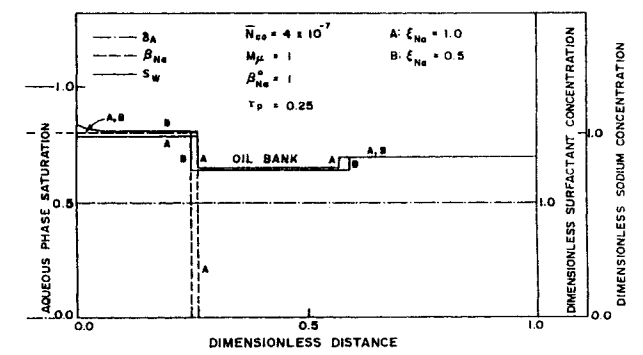


**Figure 10. Tertiary recovery profiles at different $C_{NaCl}$.**

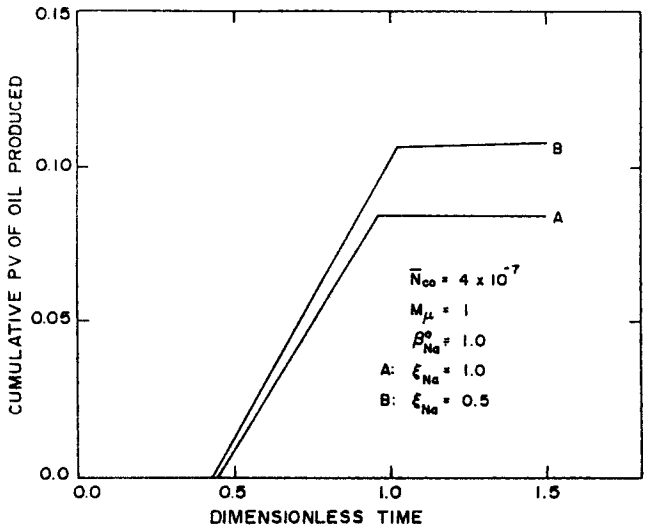


**Figure 11. Tertiary recovery cumulative oil production at different $C_{NaCl}$.**

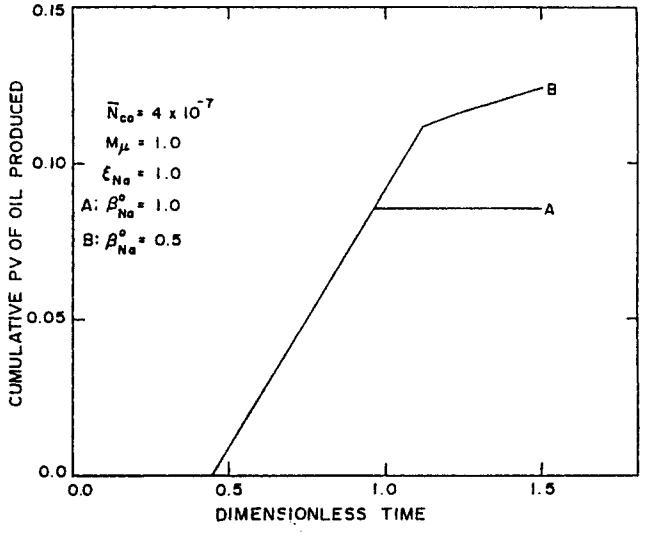


**Figure 13. Tertiary recovery cumulative oil production at different injection NaOH concentration.**

later than the one for $\xi_{Na} = 1$. These are also indicated by the cumulative oil production curves.

In the case of varying inlet NaOH concentration, oil production begins at the same time as long as $\beta^0_{Na}$ is above the $\beta_{Na}$ at the critical point. Figure 12 illustrates this for $\beta^0_{Na}s = 1.0$ and 0.5. For these two inlet concentrations of NaOH, even the rate of production due to oil bank formation is the same. But for a $\beta_{Na} = 0.5$, the oil bank is longer and hence oil production continues for a longer time. In fact, since $\beta^0_{Na} = 0.5$ is very close to the critical point, oil is produced in significant quantities even after Na breakthrough. In Figure 13 this is shown by the slightly curved line after an injection of about 1.1 pore volumes of aqueous phase.

At this stage it should be emphasized that the viscosity ratio remains a dominant parameter in determining both the *efficiency* and the *effectiveness* of the process. To show this we have plotted the profiles and histories with adsorption effects in Figures 14 and 15. Qualitatively, the profiles show the same effects as in the zero ion exchange case. From the production curves of Figure 15, however, it appears that the advantages of a higher ultimate oil recovery at lower viscosity ratios is partially lost due to adsorption. This is again because of the decreased role that the optimal region plays in determining oil recovery. However, as seen in Figure 15 adsorption appears to delay oil production more in the case of unfavorable mobility ratios.

## Conclusions

- Inclusion of mineral/alkali interactions leads to apparent nonuniqueness when the simple wave curves are analyzed; this is resolved by an analysis of discontinuity curves which in turn gives rise to a critical point. The presence of the critical point leads to simple numerical procedures for the construction of the solution.
- Reversible ion exchange leads to a delay in the chemical front whenever the NaCl or the inlet NaOH concentration is decreased. This is consistent with earlier literature.
- Adsorption reduces the influence of the optimal region in recovering oil; therefore, a faster chemical front using higher NaOH and NaCl values can actually be detrimental to ultimate oil recovery. Thus, the choice of a faster front competes with that of a higher oil recovery.

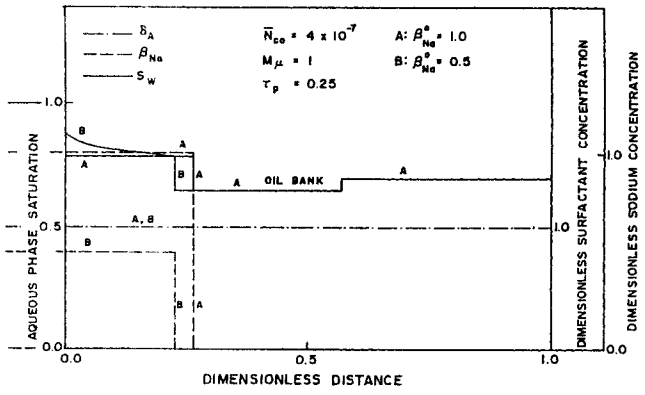


**Figure 12. Tertiary recovery profiles at different injection NaOH concentration.**

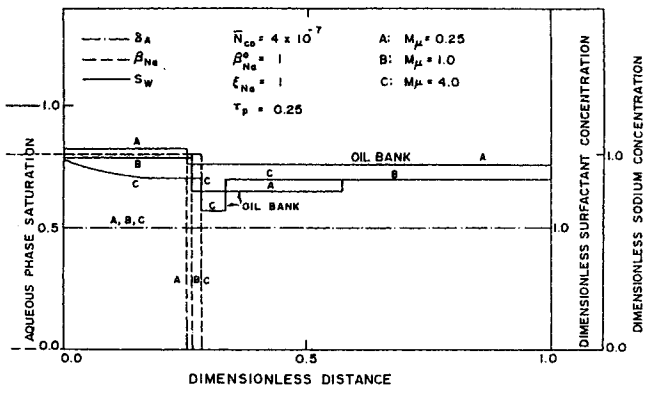


**Figure 14. Effect of viscosity ratio on tertiary recovery profiles.**

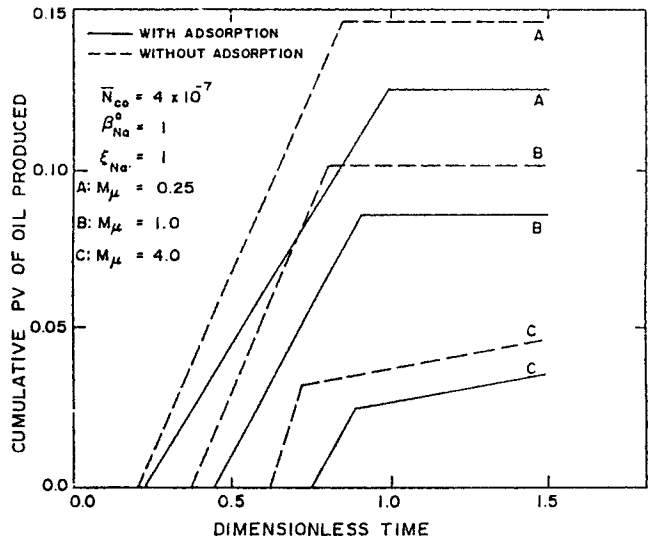


**Figure 15. Effect of viscosity ratio on tertiary recovery cumulative oil production.**

• There is a small reduction in the advantages of using a favorable mobility ratio as far as ultimate oil recovery is concerned. However, this is offset by the prediction that the commencement of oil production is affected more in the case of unfavorable viscosity ratios.

The last two conclusions imply that computation specific to a system have to be made before a choice of NaOH and NaCl concentrations is made.

## Acknowledgment

We would like to thank the Department of Energy for providing support for this work.

## Notation

$a_{C_2}$ = fitted constant as in Eq. 9
$a_{n_\infty}$ = fitted constant as in Eq. 8
$A$ = coefficient matrix
$C_{1f}$ = fixed NaOH concentration for normalization
$C_{2f}$ = fixed NaCl concentration for normalization
$C_2$ = injection concentration of NaCl
$C_e$ = electrolyte concentration
$C_{(HA_o)_0}$ = original concentration of HA in oil
$C_i$ = concentration of species $i$
$f$ = adsorbed fraction at the fluid-fluid interface
$f_w$ = fractional flow of aqueous phase
$F$ = fixed state fractional flow
$k$ = Boltzmann constant
$k_1$ = adsorption rate constant
$k_2$ = desorption rate constant
$K_A$ = acid dissociation constant
$K_D$ = acid distribution ratio
$K_r$ = Langmuir adsorption constant for Na
$K_s$ = overall salt equilibrium constant
$K_{s1}$ = salt equilibrium constant
$K_{s2}$ = salt distribution ratio
$K_w$ = dissociation constant of water
$l$ = arbitrary parameter along a wave curve
$L$ = Length of the core
$n_{A^-}$ = adsorbed $A^-$ at the fluid-fluid interface
$\bar{n}_{Na}$ = adsorbed Na per unit volume of solid
$n_{max}$ = maximum unit area adsorption at fluid-fluid interface
$\bar{n}_s$ = saturation adsorption of Na per unit volume of solid
$N$ = Avagadro number
$R$ = gas constant
$\mathbf{r}^{(i)}$ = eigenvector of family $i$
$S$ = fixed state saturation
$S^c$ = $S$ for discontinuity curve through critical point
$S_{rw}$ = residual water
$S^0_{ro,m}$ = maximum residual oil in ordinary waterflood
$S_w$ = aqueous phase saturation
$t$ = time
$T$ = temperature
$\mathbf{u}$ = dependent variable vector
$\mathbf{u}^{(k)}$ = dependent variable at some state $k$
$\mathbf{u}_s^+$ = secondary recovery initial state
$\mathbf{u}_t^+$ = tertiary recovery initial state
$V$ = overall Darcy velocity
$W$ = energy barrier for desorption
$x$ = distance from the inlet edge of the core
$z$ = dimensionless distance

### *Greek letters*

$\beta_{Na}$ = normalized sodium concentration
$\beta^0_{Na}$ = normalized injection sodium concentration
$\Gamma^{(i)}$ = simple wave curve of family $i$
$\Gamma^{(k)}$ = $k$ th simple wave curve arranged by magnitude
$\delta_A$ = normalized surface active species concentration
$\epsilon$ = electronic charge
$\epsilon_0$ = permittivity of vacuum
$\epsilon_r$ = relative permittivity of the medium
$\zeta$ = dimensionless Langmuir adsorption constant
$\eta_{Na}$ = dimensionless derivative of adsorption isotherm
$\kappa$ = dimensionless saturation adsorption
$\lambda^{(i)}$ = eigenvalue of family $i$
$\Lambda^{(i)}$ = discontinuity velocity of family $i$
$\overline{\lambda}^{(r)}$ = defined by Eq. 47
$\nu$ = solid to void volume ratio
$\xi_{Na}$ = normalized NaCl concentration
$\tau$ = dimensionless time
$\phi$ = porosity
$\psi$ = potential in the double layer

### *Subscript*

$o$ = denotes oleic phase species
$w$ = denotes water or aqueous phase species

### *Superscripts*

$p$ = denotes positive side
$m$ = denotes minus side

## Literature Cited

Bunge, A. L., "Tranport of Electrolytes in Underground Porous Media," PhD Thesis, Univ. California, Berkeley (1982).

Bunge, A. L., and C. J. Radke, "Migration of Alkaline Pulses in Reservoir Sands," *Soc. Pet. Eng. J.*, **22,** 998 (1982).

Dafermos, C. M., *Systems of Nonlinear Partial Differential Equations,* J. M. Ball, ed., Reidel Publishing, Boston (1983).

Dehghani, K., and L. L. Handy, "Caustic Consumption by a Sandstone at Elevated Temperatures," preprint SPE 12767 (1984).

deZabala, E. F., J. M. Vislocky, E. Rubin, and C. J. A. Radke, "Chemical Therapy for Linear Alkaline Flooding," *Soc. Pet. Eng. J.*, **22,** 245 (1982).

Jeffrey, A., *Quasilinear Hyperbolic Systems and Waves,* Pitman, San Francisco (1976).

Lieu, V. T., S. G. Miller, and S. A. Miller, "Laboratory Study of Chemical Reactions with Reservoir Sand in the Recovery of Petroleum by Alkaline Flooding," *Soc. Pet. Eng. J.*, **25,** 587 (1985).

Lieu, V. T., S. G. Miller, and S. J. Staphanos, *Soluble Silicates,* J. S. Falcone, ed., ACS, Washington, D. C. (1982).

Liu, T. P., "The Riemann Problem for General 2 × 2 Conservation Laws," *Trans. Am. Math. Soc.*, **199,** 89 (1974).
Mohnot, S. M., J. H. Bae, and W. L. Foley, "A Study of Mineral-Alkali Reactions," *Proc. Tech. Conf. of SPE of AIME*, SPE 13032 (1985).
Pope, G. A., "The Application of Fractional Flow Theory to Enhanced Oil Recovery," *Soc. Pet. Eng. J.*, **20,** 191 (1980).
Ramakrishnan, T. S., "Application of Fractional Flow Theory to High pH Flooding—The High pH Flooding Process," PhD Thesis, Illinois Inst. of Technol., Chicago (1985).
Ramakrishnan, T. S, and D. T. Wasan, "A Model for Interfacial Activity of Acidic Crude Oil/Caustic Systems for Alkaline Flooding," *Soc. Pet. Eng. J.*, **23,** 602 (1983).
Ramakrishnan, T. S., and D. T. Wasan, "Effect of Capillary Number on the Relative Permeability Function for Two-Phase Flow in Porous Media," *Powder Technol.*, **28,** 99 (1986).
———, "Fractional-Flow Model for High pH Flooding," *SPE Res. Eng.*, **4,** 59 (1989).
Sydansk, R. D., "Elevated-Temperature Caustic/Sandstone Interaction: Implications for Improving Oil Recovery," *Soc. Pet. Eng. J.*, **22,** 453 (1982).
Temple, B., *Contemporary Methematics: Nonlinear Partial Differential equations*, J. Smoller, ed., Vol. 17. Amer. Math. Soc., Providence, RI (1983).

*Manuscript received Aug. 25, 1989, and revision received Feb. 23, 1990.*